Squaring and Cross-Correlation Codeless Tracking: Analysis and Generalization

Daniele Borio[1], *Member, IEEE*

Abstract

In this paper, squaring and cross-correlation codeless Phase Lock Loops (PLLs) for Global Navigation Satellite Systems (GNSS) applications are at first reviewed. It is shown that the discriminators of squaring and cross-correlation PLLs are special solutions of the Maximum Likelihood (ML) equation for the estimation of the L2 P(Y) signal phase. A Generalized Codeless PLL (GCPLL), combining squaring and cross-correlation processing, is then derived as general solution of the ML equation. Approximate expressions for the tracking jitter of the considered codeless techniques are provided and validated using Monte Carlo simulations. The analysis is further supported by results obtained using live GPS L1 and L2 signals.

Index Terms

Codeless, Cross-Correlation, Global Navigation Satellite Systems, GNSS, Squaring PLL, Tracking.

I. Introduction

Professional dual-frequency Global Positioning System (GPS) receivers are able to provide measurements from both L1 and L2 signals using codeless and semi-codeless techniques. The term "codeless" [15] implies that the receiver does not need the knowledge of the signal code to extract useful measurements. In the semi-codeless case, at least a partial knowledge of the signal code is required [15]. The introduction of such techniques in the mid-90's [5] allowed one overcome the limitations imposed by the encryption of the Precision (P) code. In this respect,

1) Institute for the Protection and Security of Citizen (IPSC), Joint Research Centre (ISPRA), Italy. Email: daniele.borio@ieee.org

codeless and semi-codeless techniques were the only means of obtaining measurements from several frequencies.

Despite their use in high-end GPS receivers, codeless and semi-codeless techniques have been marginally considered by the scientific community [6], [17]. For example, [17], that provides a comprehensive overview of different codeless and semi-codeless techniques, only marginally analyzed the performance of such algorithms. The analysis provided by [17] is based on previous results from the theory of the analog Phase Lock Loop (PLL)and several results are provided without proof. In addition to this, [17] did not consider the issues implied by the implementation of such techniques on digital platforms. The results provided by [17] have been reconsidered by [6] essentially without changes.

This lack of interest is, in part, justified by the advent of new Global Navigation Satellite Systems (GNSS) that are expected to provide signals and measurements from different frequency bands thus reducing the usefulness of codeless and semi-codeless algorithms. However, delays in the deployment of new GNSS and difficulties in the modernization of existing systems still make these techniques essential for the proper functioning of professional dual-frequency receivers. In addition to this, intentional interference and spoofing make the processing of encrypted P signals a potential source of countermeasures to those threats [8]. Codeless and semi-codeless algorithms could be used for extracting signal signatures difficult to counterfeit.

For the reasons mentioned above, the main focus of this paper is the analysis and generalization of codeless techniques. Standard codeless techniques are at first reviewed with specific emphasis on squaring and cross-correlation PLLs. It is shown that the discriminators of squaring and cross-correlation PLLs are special solutions of the Maximum Likelihood (ML) equation for the estimation of the phase of the encrypted L2 P signal, denoted as P(Y) signal.

A Generalized Codeless PLL (GCPLL) is then derived as general solution of the ML equation. The proposed codeless scheme is to the best author's knowledge new and represents one of the main contributions of the paper. The GCPLL combines squaring and cross-correlation processing and provides improved performance in terms of tracking jitter and tracking threshold.

Approximate expressions for the tracking jitter of the considered techniques are provided and validated through Monte Carlo simulations. The good agreement between theoretical and simulation results supports the validity of the developed theory. Specific details are provided for the implementation of the proposed algorithms on a digital platform and live L1 and L2 P(Y) GPS

data are used to support the effectiveness of the proposed techniques.
Although the theory is developed with respect to the P(Y) code, it can be applied to different modulations, including the military M-code [2]. Cross-correlation techniques can, for example, be developed using the side-lobe components of the M-code signal.

The remainder of this paper is organized as follows. In Section II the signals and systems considered in the paper are introduced. The codeless ML phase estimator is derived in Section III whereas the GCPLL is introduced in Section IV. Section V analyzes the tracking jitter of the considered techniques; implementation details and experimental results are provided in Section VI. Finally, Section VII concludes the paper.

II. Signal and System Model

Legacy GPS satellites (block II/IIA/IIR) transmit signals in two different frequency bands: L1 with centre frequency $f_{L1} = 1575.42$ MHz and L2 with $f_{L2} = 1227.6$ MHz [6]. In the L1 band, two signals, the Coarse/Acquisition (C/A) and P codes, are broadcast in quadra-phase. The first is a civil signal accessible to the majority of users whereas the second is usually encrypted and reserved for military operations. Encryption of the military signal is achieved by modulating the known P code [6] with an unknown sequence usually denoted as W code. The combination of P and W codes leads to the encrypted signal denoted as P(Y). In the L2 band, legacy GPS satellites broadcast a single component that is the replica of the P(Y) signal broadcast in the L1 band. Thus, the signal at the input of a GPS receiver from a legacy GPS satellite can be modeled as

$$\begin{aligned} y(t) = &\sqrt{2C}d\left(t-\tau_1\right)c\left(t-\tau_1\right)\cos\left(2\pi\left(f_{L1}+f_1\right)t+\varphi_1\right) \\ &+\sqrt{2C_{p,1}}d\left(t-\tau_1\right)c_Y\left(t-\tau_1\right)\sin\left(2\pi\left(f_{L1}+f_1\right)t+\varphi_1\right)+ \\ &+\sqrt{2C_{p,2}}d\left(t-\tau_2\right)c_Y\left(t-\tau_2\right)\sin\left(2\pi\left(f_{L2}+f_2\right)t+\varphi_2\right)+\eta(t) \end{aligned} \tag{1}$$

where

- C, $C_{p,1}$ and $C_{p,2}$ are the received powers of the C/A, P(Y) L1 and L2 components
- $d(\cdot)$ is a Binary Phase Shift Keying (BPSK) signal modeling the navigation message transmitted on the three components
- $c(t)$ and $c_Y(t)$ are the pseudorandom codes used to spread the C/A and P(Y) signals

- $f_{L1} = 1575.42$ and $f_{L2} = 1227.6$ MHz are the L1 and L2 centre frequencies
- τ_i, f_i and φ_i are the code delay, Doppler frequency and phase introduced by the communication channel on the ith signal component with $i = 1, 2$
- η is an additive noise term supposed to be Gaussian and white with Power Spectral Density (PSD) $N_0/2$. The ratio between the signal power and N_0 defines the Carrier-to-Noise density power ratio, C/N_0.

Signal (1) is filtered, down-converted and digitized by the receiver front-ends. It is assumed that the receiver adopts two front-ends operating on the L1 and L2 components, respectively. It is also assumed that an In-phase/Quadrature sampling scheme [7], [12] is adopted for the signal down-conversion and digitization. In this way, the following complex time series are obtained:

$$\begin{aligned} y_1[n] &= \sqrt{C} d\left(nT_s - \tau_1\right) c\left(nT_s - \tau_1\right) \exp\left\{j2\pi f_1 n T_s + j\varphi_1\right\} \\ &\quad + \sqrt{C_{p_1}} d\left(nT_s - \tau_1\right) c_Y\left(nT_s - \tau_1\right) \exp\left\{j2\pi f_1 n T_s + j\varphi_1 - j\pi/2\right\} + \eta_1[n] \\ y_2[n] &= \sqrt{C_{p_2}} d\left(nT_s - \tau_2\right) c_Y\left(nT_s - \tau_2\right) \exp\left\{j2\pi f_2 n T_s + j\varphi_2 - j\pi/2\right\} + \eta_2[n] \end{aligned} \tag{2}$$

where T_s is the sampling interval and $f_s = 1/T_s$ the sampling frequency. $\eta_1[n]$ and $\eta_2[n]$ are two independent Gaussian processes obtained by filtering, down-converting and sampling $\eta(t)$. The independence of these noise terms is due to the fact that the receiver front-ends operate on two disjoint frequency bands. In (2), the same sampling frequency has been used for the two signal components; this choice is justified by the fact that receiver manufacturers tend to minimize hardware differences for the processing of the L1 and L2 components, minimizing inter-channel biases.

In the following, the C/A components is used only for providing initial frequency synchronization for the P(Y) components. It is assumed that the receiver is able to track the C/A signal and extract its parameters such as the Doppler frequency. It will be shown that the receiver has to remove the C/A component in order to avoid disruptive interference between the C/A and P(Y) signals on the L1 frequency. In Section VI, a simple method for removing the C/A signal and implement codeless P(Y) tracking is discussed. After the assumption that the C/A component can be effectively removed (2) becomes:

$$\begin{aligned} y_1[n] &= \sqrt{C_{p_1}} x(nT_s - \tau_1) \exp\left\{j2\pi f_1 n T_s + j\phi_1\right\} + \eta_1[n] \\ y_2[n] &= \sqrt{C_{p_2}} x(nT_s - \tau_2) \exp\left\{j2\pi f_2 n T_s + j\phi_2\right\} + \eta_2[n] \end{aligned} \tag{3}$$

where $x(nT_s - \tau_i) = d\,(nT_s - \tau_i)\, c_Y\,(nT_s - \tau_i)$ and $\phi_i = \varphi_i - j\pi/2$ with $i = 1, 2$.
It is noted that in general, several signal components from different satellites enter the receiver antenna. Since a GPS receiver is able to recover the Doppler frequency, f_1 through the processing of the L1 C/A component, it is possible to isolate each P(Y) component on the basis of its Doppler frequency. The same consideration applies to the L2 component since its Doppler frequency is approximately given by $f_2 \approx f_1 \frac{f_{L2}}{f_{L1}}$. In this way, signals from different satellites are processed independently. Under the hypothesis

$$x(nT_s - \tau_1) \approx x(nT_s - \tau_2) = z[n] \tag{4}$$

implying that the two signal components experience similar delays, (3) becomes

$$\begin{aligned} y_1[n] &= \sqrt{C_{p_1}} z[n] \exp\{j2\pi f_1 n T_s + j\phi_1\} + \eta_1[n] \\ y_2[n] &= \sqrt{C_{p_2}} z[n] \exp\{j2\pi f_2 n T_s + j\phi_2\} + \eta_2[n] \end{aligned}. \tag{5}$$

In the following, (5) will be used as basic model for the derivation of codeless tracking loops. Since, the P(Y) code is assumed to be unknown (a priori information on the P code can be used to derive semi-codeless techniques), $z[n]$ is modeled as a uniform random variable assuming value in the set $\{-1, 1\}$:

$$z[n] \sim U\{-1, 1\}. \tag{6}$$

The samples of $z[n]$ are assumed statistically independent. It is noted that $z[n]$ can be oversampled with respect to the code rate of the P component. In that case, the hypothesis of statistical independence does not hold. Statistical independence can be however obtained by including a pre-filtering and decimation stage. This corresponds to the filtering stage used in analog codeless PLLs [17] for noise reduction.

A. Maximum Likelihood Estimation and Standard Tracking Loops

Standard tracking loops are iterative algorithms that progressively minimize/maximize a specific cost function [16]. For example, in a Delay Lock Loop (DLL), the delay of the local signal replica is iteratively adjusted in order to maximize the correlation with the incoming signal. Tracking loops can be considered gradient descent/ascent algorithms where the loop discriminator is an approximation of the derivative of the cost function: when the discriminator output is driven to zero the cost function is minimized/maximized. This principle is shown in

Fig. 1 where the architecture of a standard PLL [6] is shown. The functional blocks of the PLL are related to the different operations performed by a gradient descent algorithm. This aspect has been discussed by [13], [16] that related tracking loops to Maximum A Posteriori (MAP) estimation. More specifically, it is possible to show that a PLL iteratively minimizes the square difference between the phases of the local and incoming signals. The PLL discriminator output is thus an estimate of phase difference between incoming and local signals. When the ML criterion is used to determine this phase difference, then the PLL becomes a form of MAP estimator. The standard arctangent discriminator is the Maximum Likelihood Estimator (MLE) for the residual phase difference when a single data bits is considered [6]. In [3], [4], the phase ML estimator when several data periods are considered has been determined and used to design a new class of PLLs allowing integrations longer than the data bit duration.

A PLL can thus be designed by determining at first the MLE of the residual phase difference under the specified signal model. In the next section, the MLE for the phase of the L2 P(Y) signal is determined using signal model (5). Squaring and cross-correlation codeless PLLs are then derived from the L2 P(Y) phase MLE. A generalization of these two techniques is finally obtained.

III. Codeless Maximum Likelihood Phase Estimator

In any PLL the input signal is multiplied by a local replica of the carrier. In the case of P(Y) signals, the initial frequency and phase of the local carriers can be obtained from the L1 C/A component and the signals in (5) are multiplied by

$$\begin{aligned} l_1[n] &= \exp\left\{-j2\pi\hat{f}_1 nT_s - j\hat{\phi}_1\right\} \\ l_2[n] &= \exp\left\{-j2\pi\hat{f}_2 nT_s - j\hat{\phi}_2\right\}. \end{aligned} \tag{7}$$

where $\hat{f}_1$, $\hat{f}_2$, $\hat{\phi}_1$ and $\hat{\phi}_2$ are the initial Doppler frequencies and phases estimated by the receiver. After carrier wipe-off, (5) becomes:

$$\begin{aligned} b_1[n] &= \sqrt{C_{p_1}} z[n] \exp\left\{j2\pi\Delta f_1 nT_s + j\Delta\phi_1\right\} + \tilde{\eta}_1[n] \\ b_2[n] &= \sqrt{C_{p_2}} z[n] \exp\left\{j2\pi\Delta f_2 nT_s + j\Delta\phi_2\right\} + \tilde{\eta}_2[n] \end{aligned} \tag{8}$$

where $\Delta f_i = f_i - \hat{f}_i$ and $\Delta\phi_i = \phi_i - \hat{\phi}_1$, with $i = 1, 2$. $\tilde{\eta}_1[n]$ and $\tilde{\eta}_2[n]$ are the random processes obtained by multiplying $\eta_1[n]$ and $\eta_2[n]$ by the respective local carriers. In the following, it is

assumed that $\tilde{\eta}_1[n]$ and $\tilde{\eta}_2[n]$ are two independent circular complex Gaussian random processes the real and imaginary parts of which have variance σ_1^2 and σ_2^2, respectively.

Under the assumption

$$\Delta f_i \approx 0 \qquad i = 1, 2 \tag{9}$$

Eq. (8) further simplifies to

$$\begin{aligned} b_1[n] &= \sqrt{C_{p_1}} z[n] \exp\{j\Delta\phi_1\} + \tilde{\eta}_1[n] \\ b_2[n] &= \sqrt{C_{p_2}} z[n] \exp\{j\Delta\phi_2\} + \tilde{\eta}_2[n]. \end{aligned} \tag{10}$$

In the following, codeless squaring and cross-correlation PLLs are derived from the ML estimate of $\Delta\phi_2$.

Using the hypothesis of Gaussian noise terms, the joint probability function of $b_1[n]$ and $b_2[n]$ given $z[n]$ can be expressed as

$$\begin{aligned} f(b_1[n], b_2[n]|z[n]) &= \frac{1}{(2\pi)^2\sigma_1^2\sigma_2^2} \exp\left\{ -\frac{1}{2\sigma_1^2} \left| b_1[n] - \sqrt{C_{p_1}} z[n] \exp\{j\Delta\phi_1\} \right|^2 \right\} \\ &\quad \cdot \exp\left\{ -\frac{1}{2\sigma_2^2} \left| b_2[n] - \sqrt{C_{p_2}} z[n] \exp\{j\Delta\phi_2\} \right|^2 \right\} \\ &= \frac{1}{(2\pi)^2\sigma_1^2\sigma_2^2} \exp\left\{ -\frac{1}{2} \left[\frac{|b_1[n]|^2}{\sigma_1^2} + \frac{|b_2[n]|^2}{\sigma_2^2} + \frac{C_{p_2}\sigma_1^2 + C_{p_1}\sigma_2^2}{\sigma_1^2\sigma_2^2} \right] \right\} \\ &\quad \cdot \exp\left\{ z[n] \Re\left\{ \frac{\sqrt{C_{p_1}}}{\sigma_1^2} b_1[n] \exp\{-j\Delta\phi_1\} + \frac{\sqrt{C_{p_2}}}{\sigma_2^2} b_2[n] \exp\{-j\Delta\phi_2\} \right\} \right\}. \end{aligned} \tag{11}$$

Under the hypothesis that $z[n]$ is uniformly distributed on the set $\{-1, 1\}$, the joint probability distribution of $b_1[n]$ and $b_2[n]$ becomes

$$\begin{aligned} f(b_1[n], b_2[n]) &= \frac{1}{(2\pi)^2\sigma_1^2\sigma_2^2} \exp\left\{ -\frac{1}{2} \left[\frac{|b_1[n]|^2}{\sigma_1^2} + \frac{|b_2[n]|^2}{\sigma_2^2} + \frac{C_{p_1}\sigma_2^2 + C_{p_1}\sigma_2^2}{\sigma_1^2\sigma_2^2} \right] \right\} \\ &\quad \cdot \cosh\left\{ \Re\left\{ \frac{\sqrt{C_{p_1}}}{\sigma_1^2} b_1[n] \exp\{-j\Delta\phi_1\} + \frac{\sqrt{C_{p_2}}}{\sigma_2^2} b_2[n] \exp\{-j\Delta\phi_2\} \right\} \right\}. \end{aligned} \tag{12}$$

From (12), it is possible to derive the log-likelihood function

$$\begin{aligned} \log\left[f(b_1[n], b_2[n])\right] &= -2\log\left[2\pi\sigma_1\sigma_2\right] - \frac{1}{2} \left[\frac{|b_1[n]|^2}{\sigma_1^2} + \frac{|b_2[n]|^2}{\sigma_2^2} + \frac{C_{p_1}\sigma_2^2 + C_{p_2}\sigma_2^2}{\sigma_1^2\sigma_2^2} \right] \\ &\quad + \log\cosh\left[\Re\left\{ \frac{\sqrt{C_{p_1}}}{\sigma_1^2} b_1[n] \exp\{-j\Delta\phi_1\} + \frac{\sqrt{C_{p_2}}}{\sigma_2^2} b_2[n] \exp\{-j\Delta\phi_2\} \right\} \right]. \end{aligned} \tag{13}$$

In GPS/GNSS applications, the signal components are buried in noise and the condition

$$\sigma_i^2 \gg C_{p_i} \qquad i = 1, 2 \tag{14}$$

allows the use of the approximation

$$\log\cosh(x) \approx x^2. \tag{15}$$

Thus, by removing the terms independent from $\Delta\phi_1$ and $\Delta\phi_2$ and using (15), the cost function to be maximized becomes

$$h_n\left(\Delta\phi_1, \Delta\phi_2\right) = \left(\Re\left\{ \frac{\sqrt{C_{p_1}}}{\sigma_1^2} b_1[n] \exp\left\{-j\Delta\phi_1\right\} + \frac{\sqrt{C_{p_2}}}{\sigma_2^2} b_2[n] \exp\{-j\Delta\phi_2\} \right\} \right)^2. \tag{16}$$

Finally, when L independent samples from $b_1[n]$ and $b_2[n]$ are used for the estimation of $\Delta\phi_1$ and $\Delta\phi_2$, the scaled log-likelihood function assumes the following form:

$$\begin{aligned} L\left(\Delta\phi_1, \Delta\phi_2\right) &= \sum_{n=0}^{L-1} h_n\left(\Delta\phi_1, \Delta\phi_2\right) \\ &= \sum_{n=0}^{L-1} \left(\Re\left[\frac{\sqrt{C_{p_1}}}{\sigma_1^2} b_1[n] \exp\left\{-j\Delta\phi_1\right\} + \frac{\sqrt{C_{p_2}}}{\sigma_2^2} b_2[n] \exp\{-j\Delta\phi_2\} \right] \right)^2. \end{aligned} \tag{17}$$

Codeless PLLs are designed to recover a single phase and thus an additional hypothesis is required for the simplification of (17). In particular, it is assumed that the L1 component is perfectly tracked and $\Delta\phi_1 = 0$. This hypothesis and its implications will be further discussed in Sections IV and VI. Under this hypothesis, (17) can be simplified as

$$\begin{aligned} L\left(\Delta\phi_2\right) &= L\left(0, \Delta\phi_2\right) \\ &= \sum_{n=0}^{L-1} \left(\frac{\sqrt{C_{p_1}}}{\sigma_1^2} \Re\left\{b_1[n]\right\} + \frac{\sqrt{C_{p_2}}}{\sigma_2^2} \Re\left\{b_2[n] \exp\{-j\Delta\phi_2\}\right\} \right)^2. \end{aligned} \tag{18}$$

The ML estimate of $\Delta\phi_2$ is obtained by solving

$$\frac{\partial}{\partial\Delta\phi_2} L\left(\Delta\phi_2\right) = 0. \tag{19}$$

After some manipulations, it is possible to show that (19) leads to the condition

$$\rho_s \Im\left\{P_s \exp\left\{-j2\Delta\phi_2\right\}\right\} + 2\rho_c \Im\left\{P_c \exp\left\{-j\Delta\phi_2\right\}\right\} = 0 \tag{20}$$

where

- $\rho_s = \frac{C_{p_2}}{\sigma_4^2}$ and $\rho_c = \frac{\sqrt{C_{p_1} C_{p_2}}}{\sigma_1^2 \sigma_2^2}$

- $P_s = \frac{1}{L}\sum_{n=0}^{L-1} b_2^2[n]$
- $P_c = \frac{1}{L}\sum_{n=0}^{L-1} i_1[n]b_2[n]$ with $i_1[n] = \Re\{b_1[n]\}$.

It is noted that the unknown P(Y) code is removed through squaring and cross-correlation with the real part of $b_1[n]$: the operations required for the computation of P_s and P_c are at the basis of squaring and cross-correlation codeless PLLs.

Before finding a general solution of (20), two special cases are at first considered.

A. Squaring

When $\rho_s \gg \rho_c$ or the P(Y) L1 signal is not present ($\rho_c = 0$), (20) becomes

$$\rho_s \Im\left\{P_s \exp\left\{-j2\Delta\phi_2\right\}\right\} = 0 \tag{21}$$

and the P(Y) L2 phase estimate is given by

$$\Delta\hat{\phi}_2^s = \frac{1}{2}\angle P_s = \frac{1}{2}\angle\sum_{n=0}^{L-1} b_2^2[n] = \frac{1}{2}\arctan_2\left(\Im\{P_s\}, \Re\{P_s\}\right) \tag{22}$$

where $\arctan_2(\cdot,\cdot)$ denotes the four-quadrant arctangent. A squaring PLL essentially implements the computation of (22) using an iterative approach.

B. Cross-correlation

When $\rho_c \gg \rho_s$, (20) can approximated as

$$2\rho_c \Im\left\{P_c \exp\left\{-j\Delta\phi_2\right\}\right\} = 0 \tag{23}$$

leading to

$$\Delta\hat{\phi}_2^c = \angle P_c = \angle\sum_{n=0}^{L-1} i_1[n]b_2[n] = \arctan_2\left(\Im\{P_c\}, \Re\{P_c\}\right). \tag{24}$$

This solution of the ML equation corresponds to a cross-correlation codeless PLL.

C. Generalized solution

Eq. (20) does not admit a simple closed-form solution. However, an approximated solution can be obtained by exploiting the linear approximation of the sine function. More specifically,

polar representations $P_s = |P_s| \exp\left\{j2\Delta\hat{\phi}_2^s\right\}$ and $P_c = |P_c| \exp\left\{j\Delta\hat{\phi}_2^c\right\}$ allow one to rewrite (20) as

$$\begin{aligned} &\rho_s|P_s| \sin\left(2\Delta\hat{\phi}_2^s - 2\Delta\phi_2\right) + 2\rho_c|P_c| \sin\left(\Delta\hat{\phi}_2^c - \Delta\phi_2\right) \\ &\approx 2\rho_s|P_s| \left(\Delta\hat{\phi}_2^s - \Delta\phi_2\right) + 2\rho_c|P_c| \left(\Delta\hat{\phi}_2^c - \Delta\phi_2\right) = 0. \end{aligned} \tag{25}$$

The ML P(Y) L2 phase estimate is thus given by

$$\Delta\phi_2 = \frac{\rho_s|P_s|}{\rho_s|P_s| + \rho_c|P_c|}\Delta\hat{\phi}_2^s + \frac{\rho_c|P_c|}{\rho_s|P_s| + \rho_c|P_c|}\Delta\hat{\phi}_2^c \tag{26}$$

that is a weighted combination of the squaring and cross-correlation phase estimates. When the residual phase error, $\Delta\phi_2$, is small and the post-correlation Signal to Noise Ratio (SNR) is sufficiently high, then it is possible to show that

$$\begin{aligned} \mathrm{E}\left[|P_s|\right] &\approx \mathrm{E}\left[P_s\right] = C_{p_2} \\ \mathrm{E}\left[|P_c|\right] &\approx \mathrm{E}\left[P_c\right] = \sqrt{C_{p_1}C_{p_2}}. \end{aligned} \tag{27}$$

The hypothesis of high post-integration SNR is required to assure that the signal component is dominating and $P_s, P_c > 0$. This hypothesis allows one to remove the absolute value in (27). Eq. (27) implies

$$\begin{aligned} \mathrm{E}\left[\rho_s\,|P_s|\right] &\approx \frac{C_{p_2}^2}{\sigma_2^4} \\ \mathrm{E}\left[\rho_c\,|P_c|\right] &\approx \frac{C_{p_1}C_{p_2}}{\sigma_1^2\sigma_2^2} \end{aligned} \tag{28}$$

that are scaled versions of the post-integration SNR of the squaring and cross-correlation branches. In this respect, (26) is a form of Maximal-Ratio Combining (MRC) [11] where the measurements from the squaring and cross-correlation branches are weighted according to their normalized SNR.

IV. Codeless PLLs

The ML estimators derived in Section III define the cost function to be minimized by the tracking loop. More specifically, replacing the cost function in Fig. 1 by the ML estimates (22) and (24) leads to squaring and cross-correlation codeless PLLs. This fact is shown in Fig. 2 where standard correlation and phase discrimination are replaced by the operations described in (22) and (24).

Fig. 2 shows the operations performed by a squaring PLL. In this case, however the Numerically

Controlled Oscillator (NCO) generates a carrier at the same frequency of the incoming signal. In most of the literature [6], [15], [17], squaring PLLs are required to generate a local carrier at twice the signal frequency. This is not the case if the squaring operation is performed after signal down-conversion as in Fig. 2a). The equivalence between a standard squaring PLL and the PLL in Fig. 2 can be easily proven with simple algebraic operations requiring the propagation of the carrier multiplication after squaring and the removal of the $1/2$ term in the phase discriminator. It is noted that the discriminator in Fig. 2a) can resolve phases in the range $[-\pi/2; \pi/2)$ as a standard Costa loop. In standard tracking however, the presence of a preamble in the C/A code navigation message allows one to recover half-cycle ambiguities. This is not possible in squaring codeless PLLs.

A cross-correlation codeless PLL is shown in Fig. 2b). The use of a baseband version of the L1 P(Y) signal allows one to track the L2 P(Y) phase alone and not the phase difference between the two components. In addition to this, by retaining only the real part of $b_1[n]$ a noise reduction of 3 dB is achieved. In Section VI, a squaring PLL is used to synchronize the L1 P(Y) signal and recover the $i_1[n]$ component.

It is noted that different hardware paths and L1/L2 inter-channel biases may introduce a relative delay between the L1 and L2 P(Y) components. This effect is usually compensated for using a L1-L2 delay detector [15], [17]. In the following, it is assumed that the $i_1[n]$ and $b_2[n]$ components are properly aligned and this issue is not further discussed.

In both Figs. 2a) and b) carrier aiding from L1 C/A signal is used to reduce the dynamics on the L2 P(Y) phase. $\alpha = \frac{1227.6}{1575.42} = \frac{120}{154}$ is a factor used to scale the L1 C/A Doppler estimate with respect to the L2 carrier frequency and accounts for the fact that Doppler shifts are proportional to the signal centre frequency.

A GCPLL can be obtained by combining squaring and cross-correlation processing as indicated by (26). The GCPLL comprises two branches implementing squaring and cross-correlation processing. The outputs of the two branches is then combined according to (26). A practical implementation of the GCPLL is discussed in Section VI and a detailed representation is provided in Fig. 6.

It is noted that, in general, ρ_c and ρ_s are not known and need to be estimated. A solution is provided by Eq. (28) that interprets $\rho_s|P_s|$ and $\rho_c|P_c|$ as scaled post-coherent SNRs that can be directly estimated from the outputs of the squaring and cross-correlation branches.

V. Tracking Jitter Analysis

In this section, approximate formulas for the tracking jitter of standard and generalized codeless PLLs are provided. The tracking jitter quantifies the amount of noise transfered from the input signal to the final phase estimate and can be computed as [14]

$$\sigma_\varphi = \frac{\sigma_d}{G_d}\sqrt{2B_{eq}T_c} = \frac{\sigma_d}{G_d}\sqrt{2B_{eq}LT_s} \tag{29}$$

where σ_d is the standard deviation of the discriminator output, B_{eq} is the loop equivalent bandwidth and $T_c = LT_s$ is the loop update interval. G_d is the discriminator gain defined as

$$G_d = \left.\frac{\partial \mathrm{E}\left[S(\phi)\right]}{\partial \phi}\right|_{\phi=0} \tag{30}$$

where $S(\cdot)$ is the discriminator input-output function defined by (22), (24) and (26).

In Appendix A, it is shown that the normalized variance of an arctangent discriminator, such as (22) and (24), can be approximated as

$$\frac{\sigma_d}{G_d} = \sqrt{\frac{R_x + 1}{R_x^2}} \tag{31}$$

where R_x is the post-coherent SNR of the signal at the input of the arctangent discriminator defined as

$$R_x = \frac{\left|\mathrm{E}\left[P_x\right]\right|^2}{\frac{1}{2}\mathrm{Var}\left\{P_x\right\}}. \tag{32}$$

In (31) and (32) the index 'x' is used to indicate quantities either from the squaring ($x = s$) or cross-correlation ($x = c$) branch.

For the squaring PLL

$$\begin{aligned} \mathrm{E}\left[P_s\right] &= C_{p_2}\exp\{j2\Delta\phi_2\} \\ \mathrm{Var}\left\{P_s\right\} &= 4\frac{2}{L}\left[C_{p_2}\sigma_2^2 + \sigma_2^4\right] \approx 4\frac{2\sigma_2^4}{L} \\ R_s &= \frac{C_{p_2}^2}{\frac{4}{L}\left[C_{p_2}\sigma_2^2 + \sigma_2^4\right]} \approx \frac{1}{4}\frac{LC_{p_2}^2}{\sigma_2^4} \end{aligned} \tag{33}$$

whereas the cross-correlation branch is characterized by

$$\begin{aligned} \mathrm{E}\left[P_c\right] &= \sqrt{C_{p_1}C_{p_2}}\exp\{j\Delta\phi_2\} \\ \mathrm{Var}\left\{P_c\right\} &= \frac{2}{L}\left[C_{p_1}\sigma_2^2 + \frac{1}{2}C_{p_2}\sigma_1^2 + \sigma_1^2\sigma_2^2\right] \approx \frac{2\sigma_1^2\sigma_2^2}{L} \\ R_c &= \frac{C_{p_1}C_{p_2}}{\frac{1}{L}\left[C_{p_1}\sigma_2^2 + \frac{1}{2}C_{p_2}\sigma_1^2 + \sigma_1^2\sigma_2^2\right]} \approx \frac{LC_{p_1}C_{p_2}}{\sigma_1^2\sigma_2^2} \end{aligned} \quad . \tag{34}$$

By comparing (33) and (34) with (28) it is possible to determine the scaling factors relating the mean of $\rho_s|P_s|$ and $\rho_c|P_c|$ with the post-coherent SNRs. It is noted that under the hypothesis of equal input SNRs, $\frac{C_{p_1}}{\sigma_1^2} = \frac{C_{p_2}}{\sigma_2^2}$, the post-coherent SNR of the squaring branch is reduced by a factor 4 (6 dB) with respect to the cross-correlation branch. In [17] a 3 dB gain was claimed when moving from squaring to cross-correlation codeless tracking. This difference is due to fact that in [17], cross-correlation tracking was performed by using the complex $b_1[n]$ signal and not its real part, $i_1[n]$. By removing the imaginary part of $b_1[n]$, a 3 dB gain is achieved. This type of processing is however valid only when it is possible to recover the phase of the L1 P(Y) signal.

Using (31), (33) and (34) the normalized variances of the squaring and cross-correlation discriminator outputs are finally found:

$$\frac{1}{G_d^2}\text{Var}\left\{\Delta\phi_2^s\right\} = \frac{1}{4}\frac{1}{G_d^2}\text{Var}\left\{2\Delta\phi_2^s\right\} = \frac{1}{LC_{p_2}^2/\sigma_2^4}\left(1 + \frac{4}{LC_{p_2}^2/\sigma_2^4}\right) \tag{35}$$

and

$$\frac{1}{G_d^2}\text{Var}\left\{\Delta\phi_2^c\right\} = \frac{1}{LC_{p_1}C_{p_2}/\left(\sigma_1^2\sigma_2^2\right)}\left[1 + \frac{1}{LC_{p_1}C_{p_2}/\left(\sigma_1^2\sigma_2^2\right)}\right]. \tag{36}$$

Finally, the tracking jitter for the squaring and cross-correlation PLLs assumes the following forms:

$$\sigma_\varphi^s = \sqrt{\frac{2B_{eq}T_s}{C_{p_2}^2/\sigma_2^4}\left(1 + \frac{4}{LC_{p_2}^2/\sigma_2^4}\right)} \tag{37}$$

$$\sigma_\varphi^c = \sqrt{\frac{2B_{eq}T_s}{C_{p_1}C_{p_2}/\left(\sigma_1^2\sigma_2^2\right)}\left[1 + \frac{1}{LC_{p_1}C_{p_2}/\left(\sigma_1^2\sigma_2^2\right)}\right]}. \tag{38}$$

Assuming equal noise variances, $\sigma_1^2 = \sigma_2^2$, and considering an ideal front-end filter, i.e., the receiver front-end bandwidth is equal to half the sampling frequency, it is possible to express the noise powers as

$$\sigma_1^2 = \sigma_2^2 = \frac{N_0 f_s}{2} = \frac{N_0}{2T_s}. \tag{39}$$

Under this hypothesis, the tracking jitter for the squaring and cross-correlation PLLs can be finally expressed as

$$\sigma_\varphi^s = \sqrt{\frac{B_{eq}}{2\left(\frac{C_{p_2}}{N_0}\right)^2 T_s}\left[1 + \frac{1}{\left(\frac{C_{p_2}}{N_0}\right)^2 T_s T_c}\right]} \tag{40}$$

TABLE I

PARAMETERS ADOPTED FOR THE EVALUATION OF THE TRACKING JITTER BY MONTE CARLO SIMULATIONS.

Parameter	Value
Sampling Frequency	$f_s = 40$ MHz
Intermediate Frequency	0 MHz
PLL order	2nd
Sampling Type	Complex
No. of Simulation Runs	10^5

and

$$\sigma_{\varphi}^{c} = \sqrt{\frac{B_{eq}}{2\left(\frac{C_{p_1}}{N_0}\right)\left(\frac{C_{p_2}}{N_0}\right)T_s}\left[1 + \frac{1}{4\left(\frac{C_{p_1}}{N_0}\right)\left(\frac{C_{p_2}}{N_0}\right)T_c T_s}\right]}. \tag{41}$$

The tracking jitter of the GCPLL derived in Section IV is a weighted combination of (37) and (38). More specifically, using (26) and (28), it is possible to show that the tracking jitter of the GCPLL is given by

$$\sigma_{\varphi} = \sqrt{\left[\frac{C_{p_2}/\sigma_2^2}{C_{p_1}/\sigma_1^2 + C_{p_2}/\sigma_2^2}\sigma_{\varphi}^{s}\right]^2 + \left[\frac{C_{p_1}/\sigma_1^2}{C_{p_1}/\sigma_1^2 + C_{p_2}/\sigma_2^2}\sigma_{\varphi}^{c}\right]^2}. \tag{42}$$

The advantage of the GCPLL with respect to standard codeless processing becomes evident when the C/N_0s of the L1 and L2 P(Y) components are the same. In that case, the GCPLL provides a maximal noise reduction that leads to a tracking jitter approximately $1/\sqrt{2}$ lower than the tracking jitter of squaring and cross-correlation PLLs.

A. Simulation Analysis

In order to support the theoretical results provided in Section V, Monte Carlo simulations have been used to estimate the tracking jitter under different operating conditions. The simulation parameters are summarized in Table I. Sample simulation results are provided in Figs. 3 and 4 that show the tracking jitter for the squaring, cross-correlation and generalized codeless PLLs as a function of the input C/N_0. In both figures, the L2 and L1 P(Y) signals are characterized by the same C/N_0. The good match between simulations and theoretical findings supports the validity of the theory developed in Section V.

Vertical lines in Figs. 3 and 4 indicate the C/N_0 levels at which a PLL loses lock. The squaring

PLL is more subject to loss of lock whereas the GCPLL not only provides an improved tracking jitter but is able to maintain lock for lower C/N_0 values with respect to standard codeless tracking techniques.

VI. Practical Implementation and Experimental Results

In Section II, the L1 C/A component was neglected and the ML phase estimator for the L2 P(Y) signal was derived by assuming that the phase of the L1 P(Y) component was known. In practice, dedicated processing is required to guarantee that these conditions are verified. In this section, a practical implementation of the GCPLL is detailed including the processing required to recover the L1 P(Y) component used in the cross-correlation branch. Results obtained using live GPS signals showing the effectiveness of the proposed implementation are provided at the end of the section.

In order to implement cross-correlation processing, a baseband version of the L1 P(Y) component has to be recovered. The processing scheme adopted for this purpose is shown in Fig. 5 where standard tracking loops [6] are used to recover the L1 C/A component. A DLL employing Early, Prompt and Late correlators is adopted to recover the code delay of the C/A component whereas a standard Costas loop [6] is used to determine the signal Doppler frequency and carrier phase. The Costas loop is also used to bring to baseband the L1 signal, including the L1 P(Y) component. The estimated Doppler frequency will be used for carrier aiding in the L2 P(Y) processing. The C/A Prompt correlator is also employed for estimating the amplitude of the C/A signal that is removed through Successive Interference Cancellation (SIC) [9]. SIC is required in order to avoid destructive interference between C/A and L1 P(Y) components. More specifically, the two signals are transmitted in quadrature and they would cancel out after squaring. Without SIC squaring would make the two components have a phase difference equal to 180 degrees resulting in signal cancellation. The outputs of the loop in Fig. 5 are a baseband version of the L1 P(Y) signal and an estimate of the signal Doppler frequency.

The processing of the P(Y) signals is shown in Fig. 6: a squaring PLL is used to recover the residual phase of the baseband L1 P(Y) signal the real part of which is used for despreading the L2 P(Y) component. The L2 P(Y) signal is tracked using the GCPLL described above. The Doppler estimate from the C/A code is scaled by the factor $\alpha = \frac{1227.6}{1575.42} = \frac{120}{154}$ and used to aid the processing of the L2 component.

It is noted that for the implementation of the GCPLL discriminator an estimate of the post-correlation SNR of the squaring and cross-correlation components is required. This is achieved by using simple exponential filters. More specifically, R_s and R_c in (33) and (34) are estimated as

$$\hat{R}_x = \frac{\left|\bar{P}_x\right|^2}{\frac{1}{2}\left[\bar{P}_{2,x} - \left|\bar{P}_x\right|^2\right]} \tag{43}$$

where $x = \{s, c\}$. In (43), $\bar{P}_x$ and $\bar{P}_{2,x}$ are estimates of the first and second moments of the complex correlator output, P_x. More specifically, $\bar{P}_x$ and $\bar{P}_{2,x}$ are obtained by applying an exponential filter to P_x and $|P_x|^2$:

$$\begin{aligned} \bar{P}_x[k] &= (1-\beta)\bar{P}_x[k-1] + \beta P_x[k] \\ \bar{P}_{2,x}[k] &= (1-\beta)\bar{P}_{2,x}[k-1] + \beta\left|P_x[k]\right|^2 \end{aligned} \tag{44}$$

where $\beta \in (0, 1]$ is the forgetting factor controlling the cut-off frequency of the filter transfer function. In the implementation considered in the paper $\beta = 0.9$. In (44), an index k has been added to denote correlators from different time epochs. $\hat{R}_s$ and $\hat{R}_c$ are then properly scaled in order to obtain the coefficients for weighting the contributions of the squaring and cross-correlation branches.

A. Real Data Analysis

In order to further support the feasibility and effectiveness of the proposed algorithms, live GPS L1 and L2 data have been collected using a National Instruments (NI) data acquisition system equipped with two PXI-5660 vector signal analyzers [10] able to operate in synchronous mode. Synchronous wideband GPS L1 and L2 signals have been collected using the NI system configured according to the settings reported in Table II. After initial acquisition from the L1 C/A component, the P(Y) L1 and L2 signals have been processed according to the tracking scheme described in Section VI and the parameters reported in Table II.

Sample results obtained by processing the collected data are shown in Figs. 7 and 8. In this case, a 200 ms integration time and a 1 Hz loop bandwidth were adopted for the processing of the P(Y) components. Doppler aiding provided by the L1 C/A component allows the use of a narrow bandwidth that is required to reduce the noise impact and assure the loop stability in the presence of long integration times. The correlator outputs from the cross-correlation and squaring

TABLE II

SETTINGS ADOPTED FOR THE COLLECTION AND PROCESSING OF WIDEBAND LIVE GPS L1 AND L2 SIGNALS.

Parameter	Value
Sampling frequency	$f_s = 25$ MHz
Sampling type	Complex
L1 intermediate frequency	0.42 MHz
L2 intermediate frequency	0.60 MHz
P(Y) integration time	200 ms
P(Y) loop bandwidth	1 Hz
P(Y) loop order	2nd

branches of the GCPLL are shown as function of time in Fig. 7. After an initial transient, the signal components are properly aligned in the in-phase part of the correlator output. From Fig. 7, it is possible to note that the cross-correlation branch produces less noisy correlator outputs than the squaring branch. This is not only due to the different processing, but also to the different signal powers recovered for the L1 and L2 P(Y) components $\left(\frac{C_{p,1}}{\sigma_1^2} \neq \frac{C_{p,2}}{\sigma_2^2}\right)$. More specifically, the antenna used for the data collection provides a higher gain in the GPS L1 band.

The different quality of the correlators produced by the two processing branches is reflected in the weights used for the computation of the generalized codeless discriminator. The weights estimated using the approach described in the first part of this section are shown in the bottom part of Fig. 8. In this case, the cross-correlation component is weighted 2 times more than the squaring contribution. For this reason, the discriminator output produced by the GCPLL is only marginally better than the one provided by a cross-correlation codeless PLL. This fact clearly emerges from the top part of Fig. 8 that shows the discriminator output of the three different codeless PLLs considered in this paper.

Results similar to those shown in Figs. 7 and 8 have been obtained for the different satellite signals present in the collected dataset. These results support the effectiveness of the considered codeless techniques.

VII. CONCLUSIONS

In this paper, squaring and cross-correlation codeless PLLs have been obtained as special solutions of the ML equation for the estimation of the L2 P(Y) signal phase. A general solution

for the ML equation has been provided and used for the design of a generalized codeless PLL combining squaring and cross-correlation processing. The proposed technique provides a reduction in tracking jitter and improved lock capabilities with respect to traditional codeless techniques.

Approximate expressions for the tracking jitter of the considered codeless techniques have been derived and validated using Monte Carlo simulations. The good agreement between theoretical and simulation results supports the validity of the developed theory. The analysis has been further supported by experiments performed using live GPS L1 and L2 signals that confirm the effectiveness of the proposed implementation of codeless techniques.

The theory developed for codeless techniques can be directly extended to the semi-codeless case by considering the pre-filtering stage used to integrate the received signal over the duration of a single chip of the W code.

APPENDIX A
ARCTANGET DISCRIMINATOR OUTPUT VARIANCE

In this appendix, the proof of (31) is briefly sketched. Consider a complex random variable

$$P_x = I_x + jQ_x = A\exp\{j\theta_x\} + \eta_x \tag{45}$$

with independent and identically distributed real and imaginary parts with variance σ_x^2 and define R_x as in (32). The output of an arctangent discriminator is defined as

$$\hat{\theta}_x = \arctan_2\left(Q_x, I_x\right). \tag{46}$$

In order to determine (31), the following approximations based on Euler's expansion [1] for the arctangent function can be used:

$$\arctan_2\left(Q_x, I_x\right) \approx \frac{I_x Q_x}{I_x^2 + Q_x^2} \approx \frac{I_x Q_x}{\mathrm{E}\left[I_x^2 + Q_x^2\right]}. \tag{47}$$

Using (47), the following properties can be easily determined

$$\begin{aligned} \mathrm{E}\left[\hat{\theta}_x\right] &\approx \frac{\frac{1}{2}A^2\sin(2\theta_x)}{A^2 + 2\sigma_x^2} \\ G_d = \left.\frac{\partial \mathrm{E}\left[\hat{\theta}_x\right]}{\partial\theta_x}\right|_{\theta_x=0} &\approx \frac{A^2}{A^2 + 2\sigma_x^2} \\ \sigma_d^2 = \mathrm{Var}\left\{\hat{\theta}_x\right\} &\approx \frac{A_x^2\sigma_x^2 + \sigma_x^4}{\left(A^2 + 2\sigma_x^2\right)^2}. \end{aligned} \tag{48}$$

Using (48), property (31) is found

$$\frac{\sigma_d}{G_d} = \sqrt{\frac{\text{Var}\left\{\hat{\theta}_x\right\}}{G_d^2}} \approx \sqrt{\frac{A_x^2\sigma_x^2 + \sigma_x^4}{A^4}} = \sqrt{\frac{\frac{A_x^2}{\sigma_x^2} + 1}{\left(\frac{A^2}{\sigma_x^2}\right)^2}} = \sqrt{\frac{R_x + 1}{R_x^2}}. \tag{49}$$

REFERENCES

[1] Abramowitz, M. and Stegun, I. A., eds.: *Handbook of Mathematical Functions: with Formulas, Graphs, and Mathematical Tables*. Dover Publications, June 1965.

[2] Barker, B. C., Betz, J. W., Clark, J. E., Correia, J. T., Gillis, J. T., Lazar, S., Rehborn, K. A., and Straton, J. R.: 'Overview of the GPS M code signal'. In *Proc. of the National Technical Meeting of The Institute of Navigation*. Anaheim, CA, Jan. 2000.

[3] Borio, D. and Lachapelle, G.: 'A non-coherent architecture for GNSS digital tracking loops'. *Annals of Telecommunications*, vol. 64 pp. 601–614, 2009.

[4] Borio, D., Sokolova, N., and Lachapelle, G.: 'Memory discriminators for non-coherent integration in GNSS tracking loops'. In *Proc. of the European Navigation Conference ENC'09*. Naples, Italy, May 2009.

[5] Dunn, C. E., Jefferson, D. C., Lichten, S. M., Thomas, J. B., Vigue, Y., and Young, L. E.: 'Time and position accuracy using codeless GPS'. In *Proc. of the 25th Precise Time and Time Interval (PTTI) Conference*. Marina del Rey, CA, Dec 1993.

[6] Kaplan, E. D. and Hegarty, C. J., eds.: *Understanding GPS: Principles and Applications*. Artech House Publishers, Norwood, MA, US, 2nd ed., 2005.

[7] Linden, D. A.: 'A discussion of sampling theorems'. *Proc. of the IRE*, vol. 47, no. 7 pp. 1219–1226, Jul. 1959.

[8] Lo, S., De Lorenzo, D., Enge, P., Akos, D., and Bradley, P.: 'Signal authentication: A secure civil GNSS for today'. *Inside GNSS*, pp. 30–39, Sep./Oct. 2009.

[9] Madhani, P., Axelrad, P., Krumvieda, K., and Thomas, J.: 'Application of successive interference cancellation to the GPS pseudolite near-far problem'. *IEEE Trans. Aerosp. Electron. Syst.*, vol. 39, no. 2 pp. 481–488, Apr. 2003.

[10] National Instruments Corporation, http://www.ni.com/pdf/products/us/4mi469-471.pdf: *2.7 GHz RF Signal Analyzer NI PXI-5660*, 2008.

[11] Simon, M. K. and Alouini, M.-S.: *Digital Communication over Fading Channels*. Wiley-Interscience, 2nd ed., 2005.

[12] Tsui, J. B.-Y.: *Fundamentals of Global Positioning System Receivers: A Software Approach*. Wiley-Interscience, 2nd ed., Dec. 2004.

[13] Tufts, D. and Francis, J.: 'Estimation and tracking of parameters of narrow-band signals by iterative processing'. *IEEE Trans. Inform. Theory*, vol. 23, no. 6 pp. 742 – 751, nov 1977.

[14] Van Dierendonck, A.: *Global Positioning System Theory and Application*, vol. 1, chap. 5, GPS Receivers, pp. 329–407. American Institutr of Aeronautics & Astronautics, 1996.

[15] Van Dierendonck, A. J.: 'Understanding GPS receiver technology: A tutorial on what those words mean'. In *Proc. of the International Symposium on Kinematic Systems in Geodesy, Geomatics and Navigation KIS94*, pp. 15–24. Banff, AB, Canada, Aug-Sep 1994.

[16] Viterbi, A. J.: *Principles of coherent communication*. McGraw-Hill, 1st ed., 1966.

[17] Woo, K. T.: 'Optimum semi-codeless carrier phase tracking of L2'. In *Proc. of the ION/GPS*, pp. 289–306. Nashville TN, US, Sep. 1999.

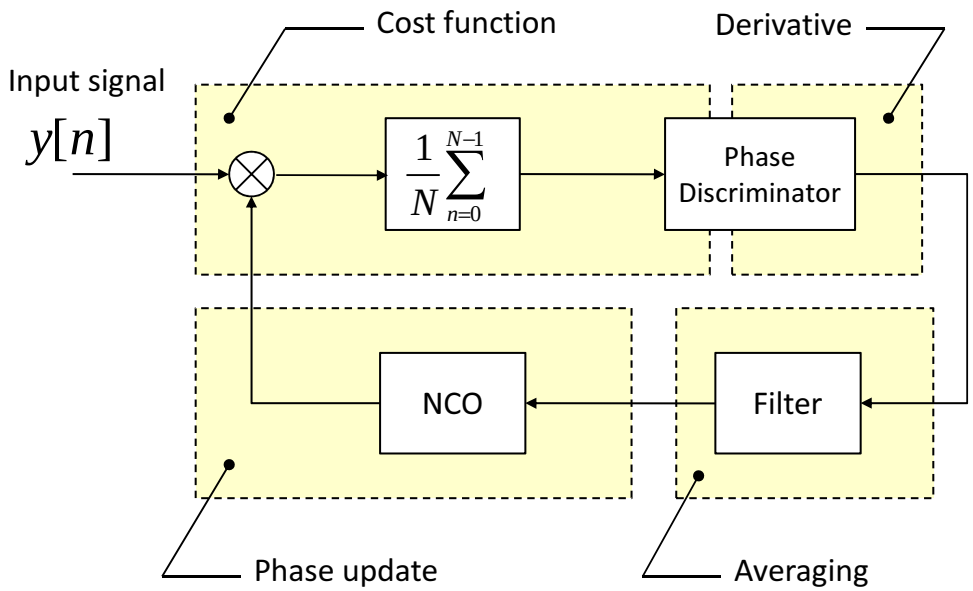

Fig. 1. Standard tracking loop interpreted as a gradient descent/ascent algorithm used for the minimization/maximization of a cost function. In a PLL, the cost function to be minimized is the square difference between the phases of the incoming and local signals.

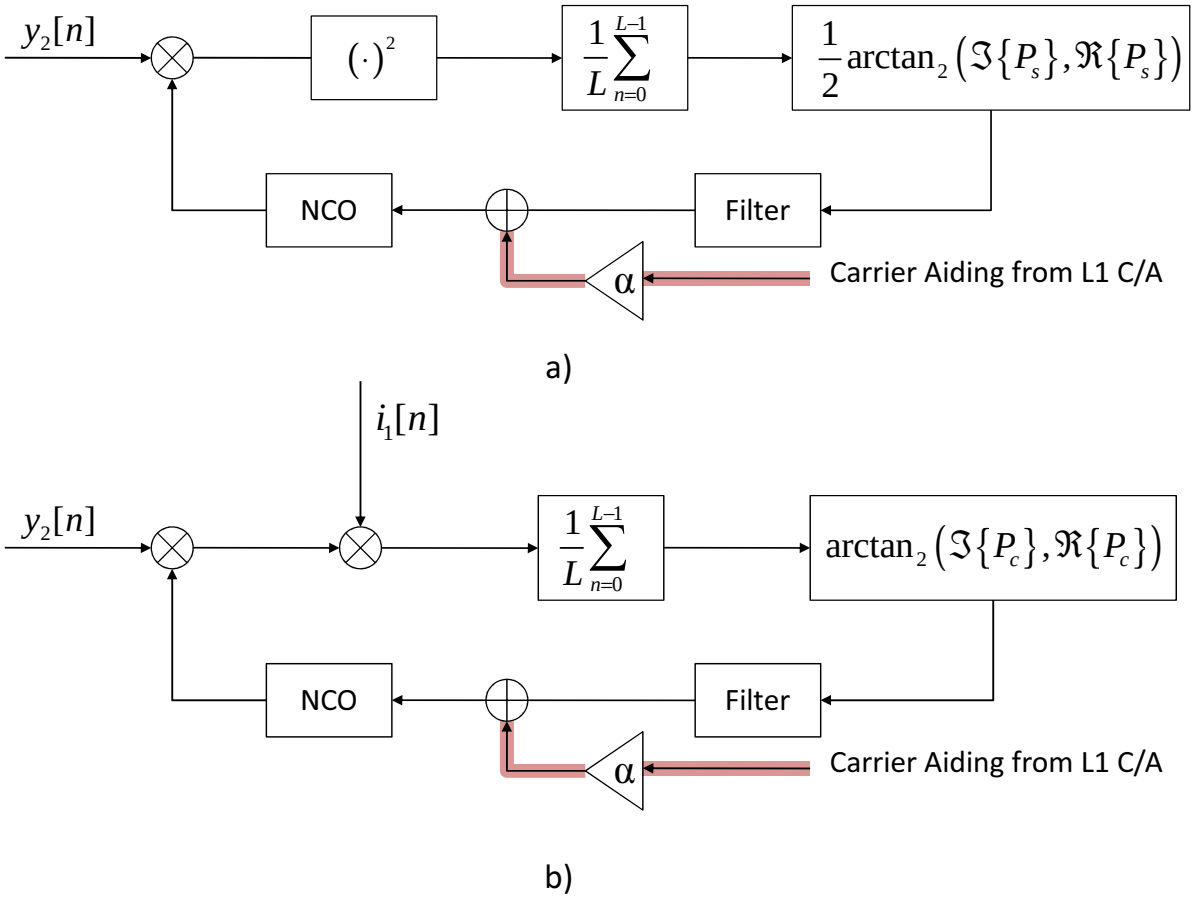

Fig. 2. Codeless PLLs derived from the ML phase estimator. a) Squaring PLL. b) Cross-correlation PLL.

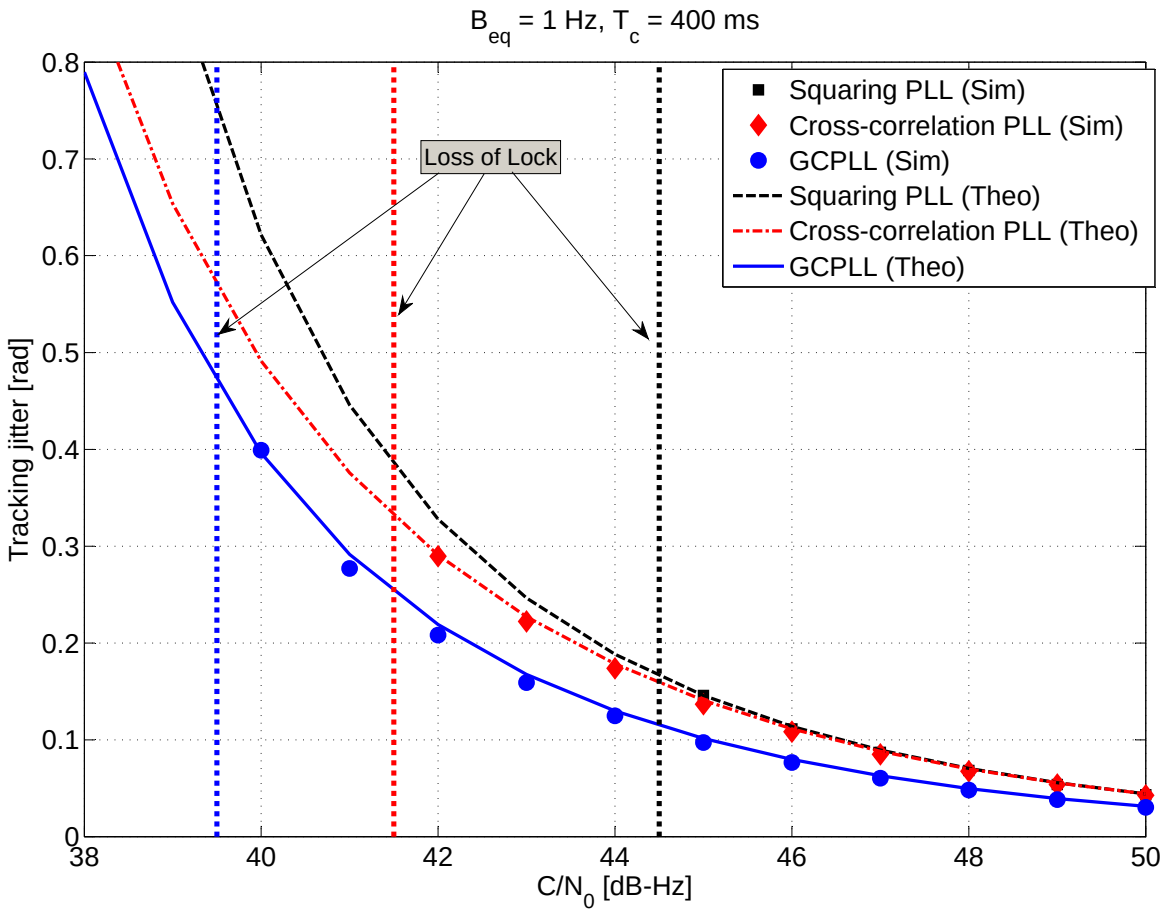

Fig. 3. Tracking jitter for squaring, cross-correlation and generalized codeless PLLs as a function of the input C/N_0. The L2 and L1 P(Y) signals are characterized by the same C/N_0. Vertical lines indicate the C/N_0 at which a PLL loses lock. Integration time, $T_c = 400$ ms.

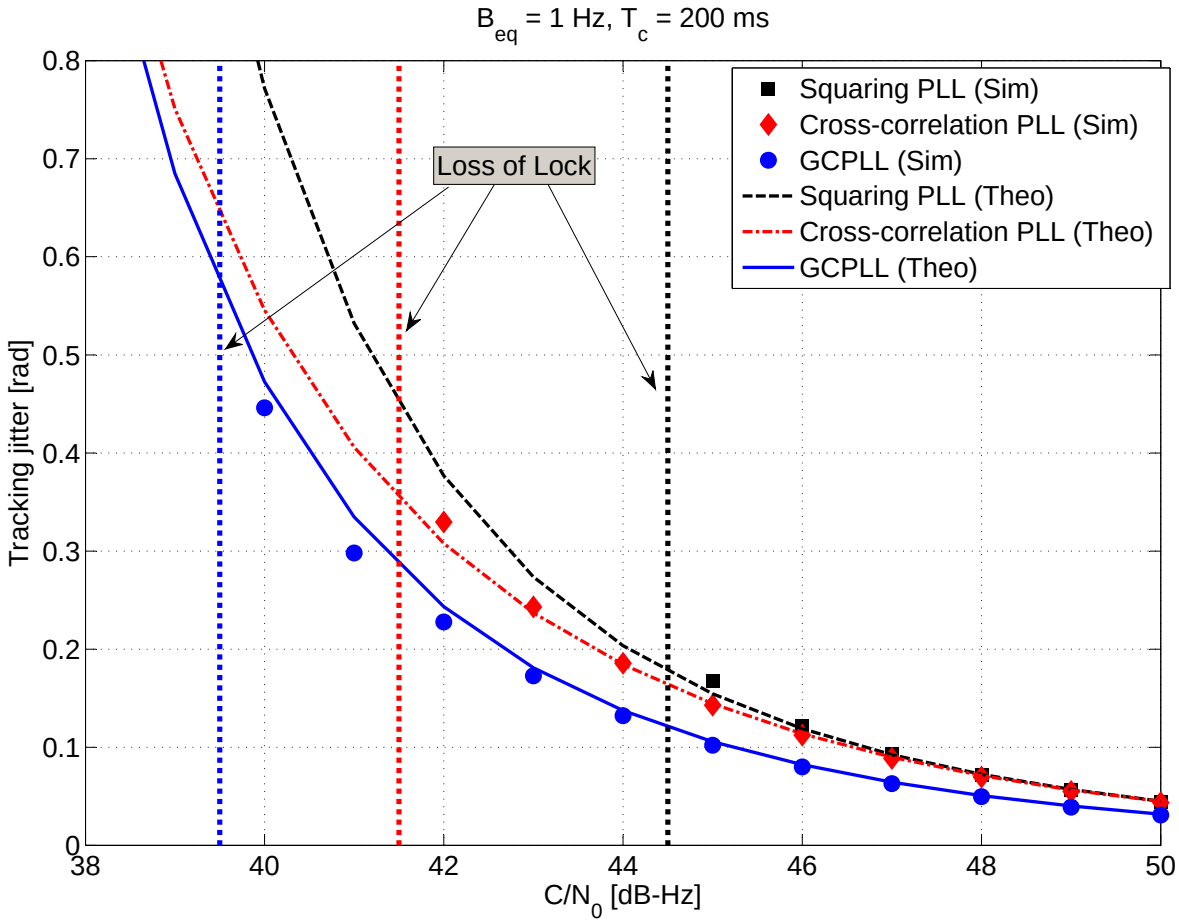

Fig. 4. Tracking jitter for squaring, cross-correlation and generalized codeless PLLs as a function of the input C/N_0. The L2 and L1 P(Y) signals are characterized by the same C/N_0. Vertical lines indicate the C/N_0 at which a PLL loses lock. Integration time, $T_c = 200$ ms.

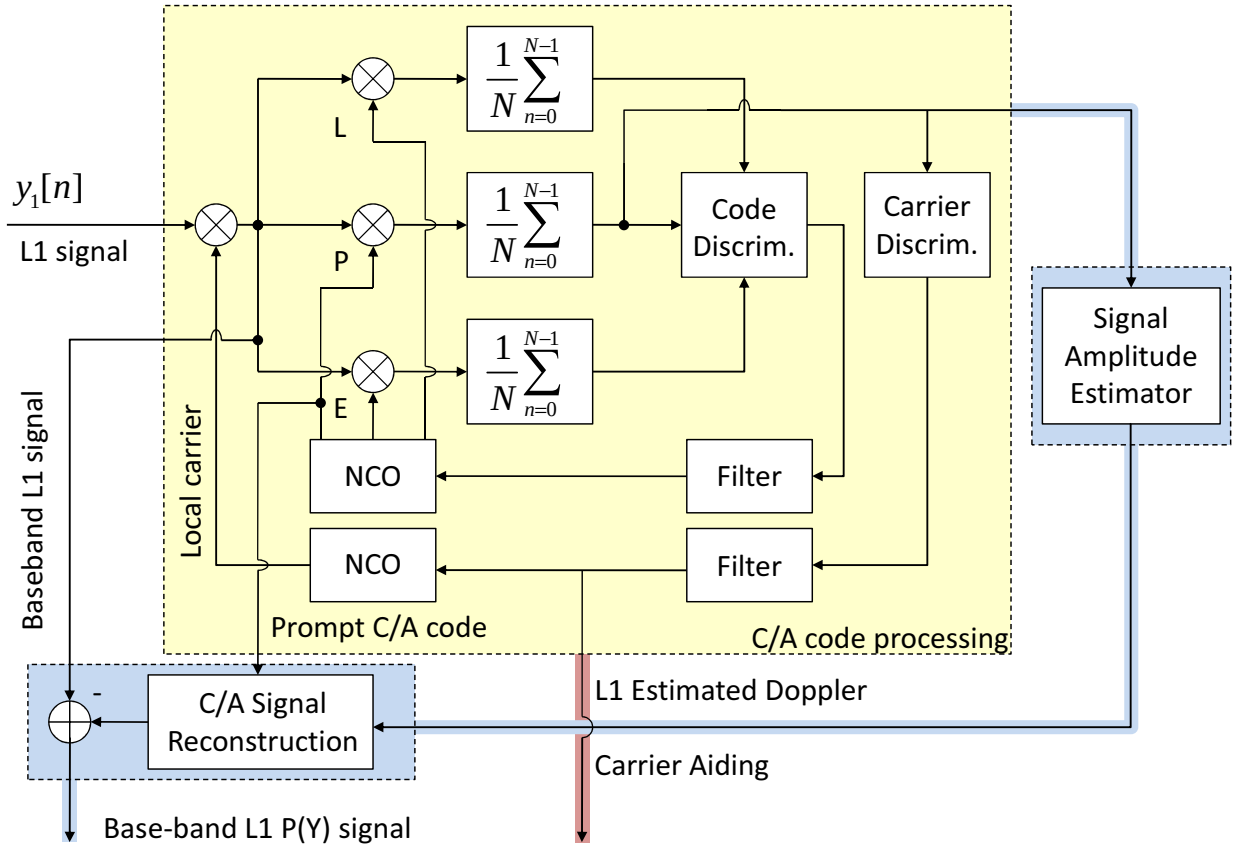

Fig. 5. Processing of the L1 components: the C/A component is used to determine a reference Doppler frequency and generate a baseband P(Y) L1 signal. The C/A signal is removed through SIC.

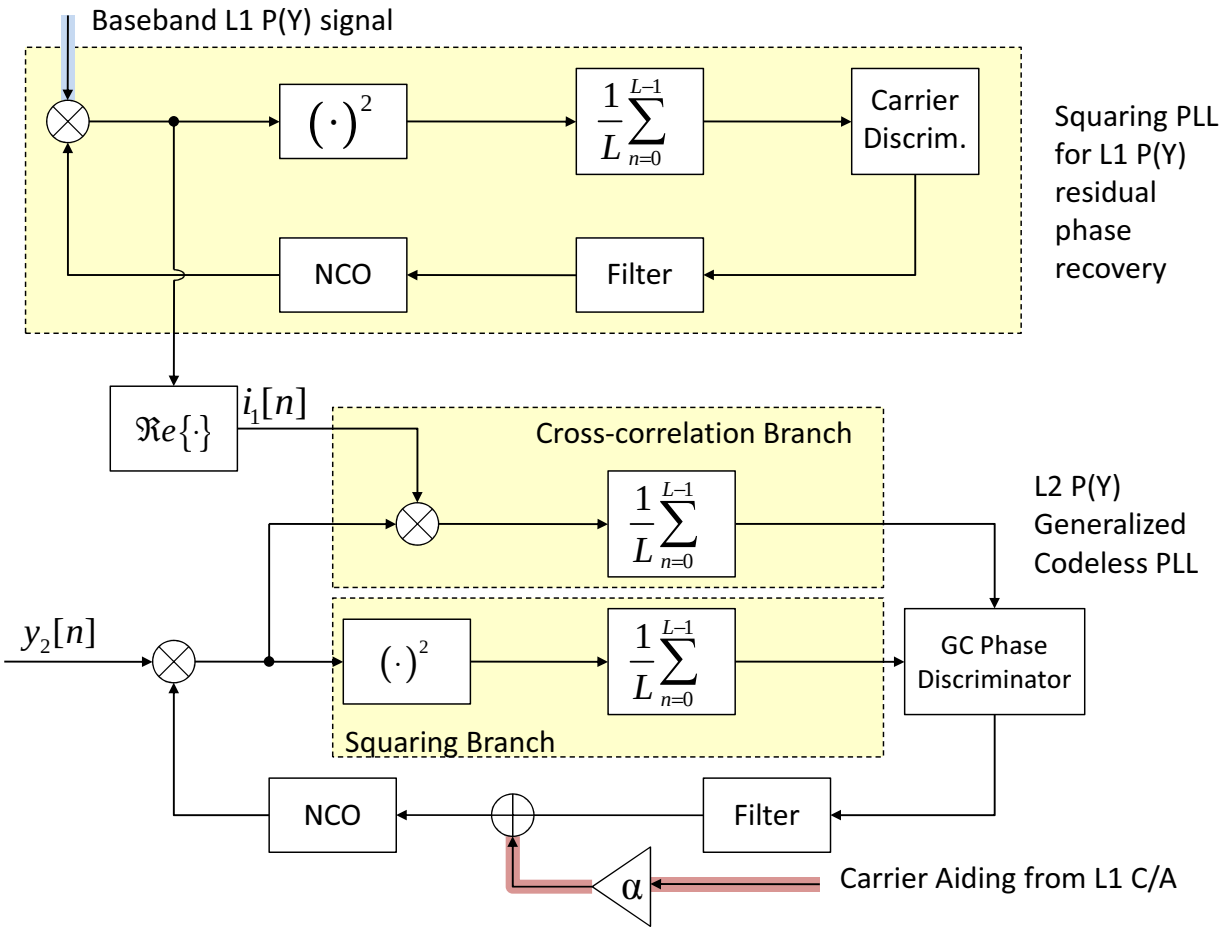

Fig. 6. Processing of the P(Y) signals: a squaring PLL is used to recover the residual phase of the baseband L1 P(Y) signal the real part of which is used for the despreading of the L2 P(Y) component. The L2 P(Y) signal is tracked using the generalized codeless PLL combining cross-correlation and squaring processing.

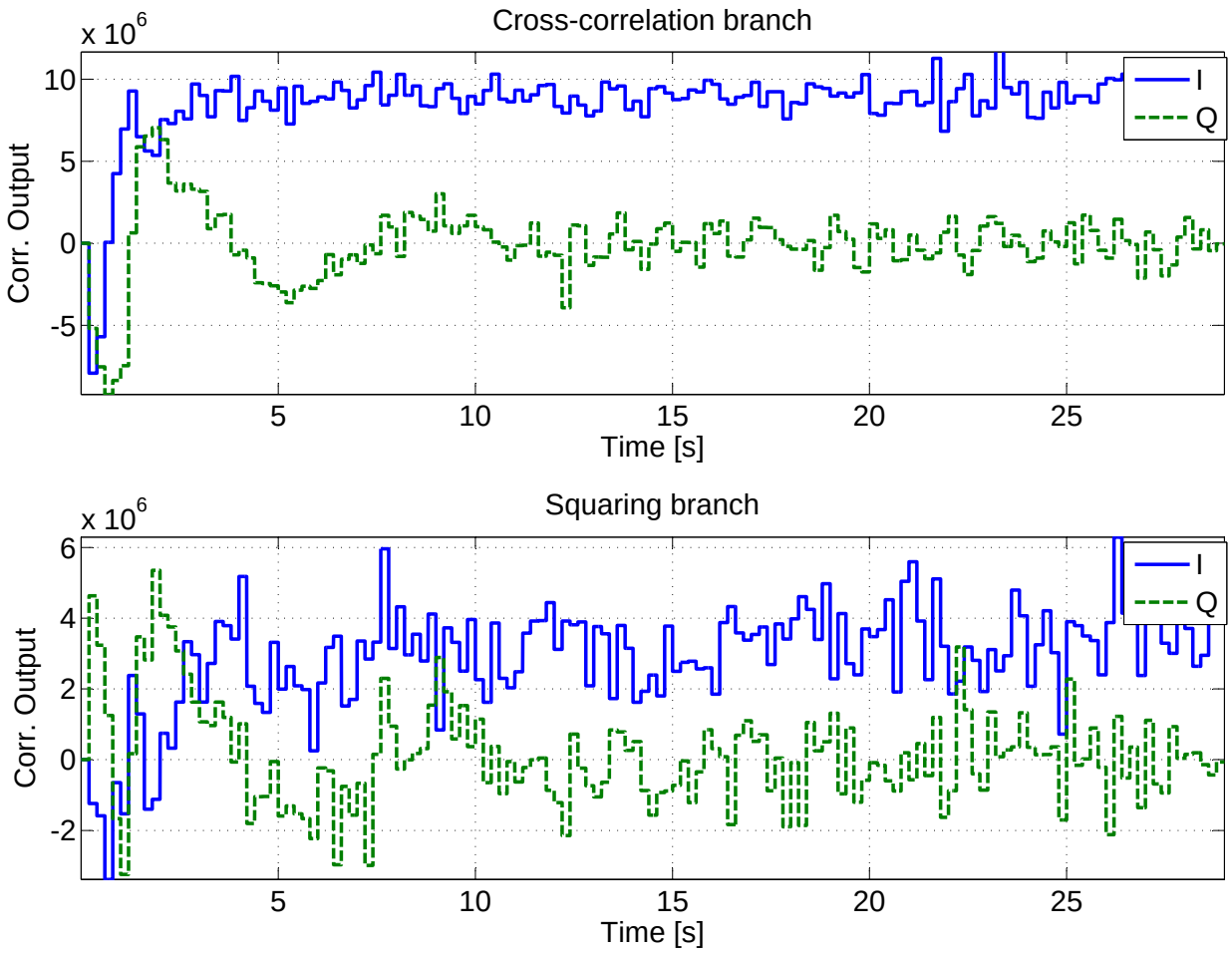

Fig. 7. Correlator outputs from the cross-correlation and squaring branches. GCPLL with a 200 ms integration time and 1 Hz bandwidth.

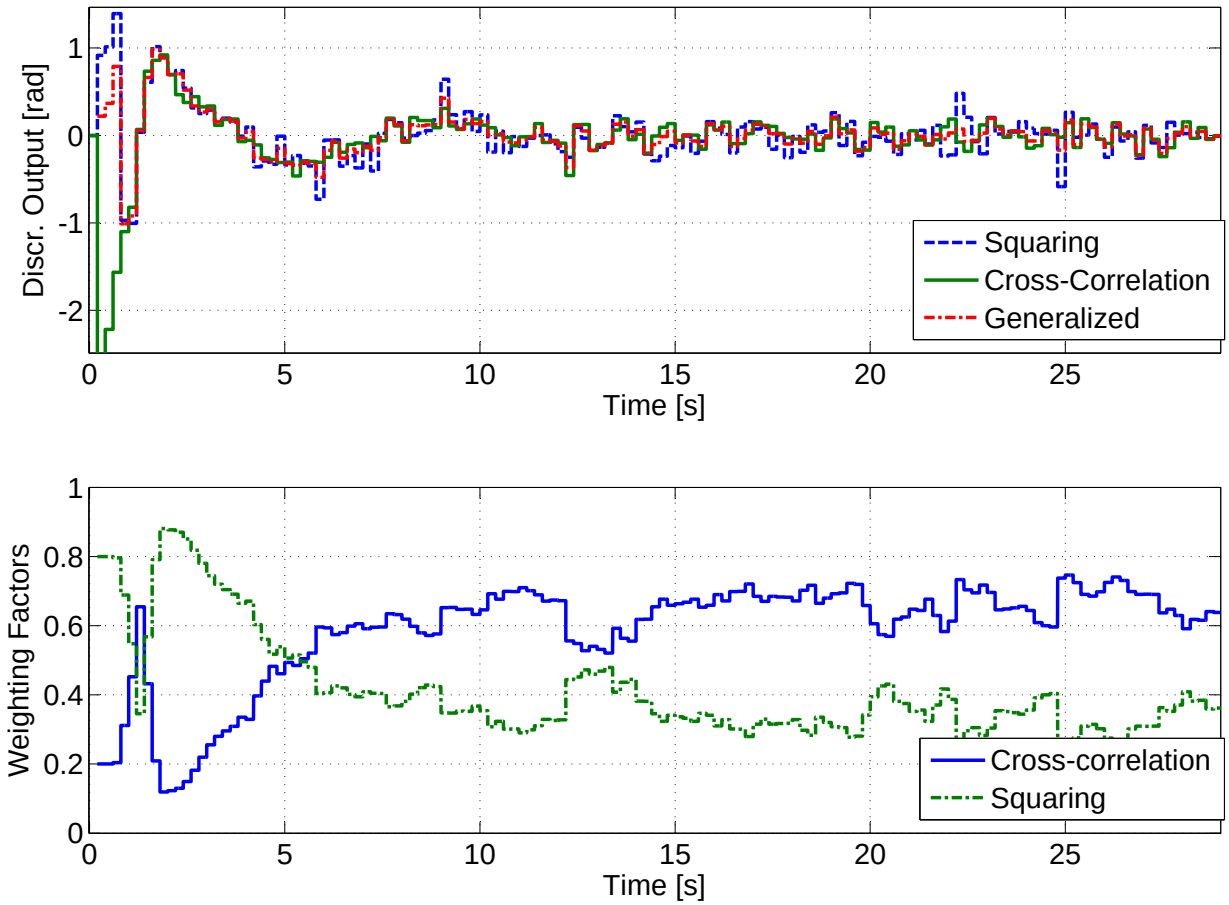

Fig. 8. Discriminator outputs and relative weights used for the computation of the generalized codeless discriminator. GCPLL with a 200 ms integration time and 1 Hz bandwidth.